

Proceedings of the Second Annual LHCP  
October 26, 2021

## Charmless B decays at LHCb

ROBERTA CARDINALE

*On behalf of the LHCb Experiment,  
Department of Physics  
University of Genova, Genova, Italy*

### ABSTRACT

The study of charmless  $b$ -hadron decays provides information for testing the CKM picture of CP violation in the Standard Model. In addition, as they can proceed through loop diagrams, they are also sensitive to physics beyond the Standard Model. A review of recent results from LHCb on charmless  $b$ -hadron decays is presented.

### PRESENTED AT

The Second Annual Conference  
on Large Hadron Collider Physics  
Columbia University, New York, U.S.A  
June 2-7, 2014

# 1 Introduction

Charmless  $b$ -hadron decays play a central role testing ground for the Standard Model. Recent results using data collected in 2011 at the LHCb detector [1] at  $\sqrt{s} = 7$  TeV, corresponding to an integrated luminosity of  $\sim 1 \text{ fb}^{-1}$ , are presented.

## 2 Search for $\Lambda_b^0(\Xi_b^0) \rightarrow K_s^0 p h^-$

The study of  $b$ -baryons decays is almost an unexplored field. Hadronic three-body  $b$ -baryons decays to charmless final states, which have not been observed yet, can provide the possibility to study hadronic decays and to search for CP violation. In these proceedings are presented the branching fractions measurements of beauty baryons decays to the final states  $K_s^0 p \pi^-$  and  $K_s^0 p K^-$ , determined relative to the  $B^0 \rightarrow K_s^0 \pi^+ \pi^-$  decay used as normalisation channel [2]. Each  $b$ -hadron decay is reconstructed by combining two charged tracks with a  $K_s^0$  candidate. The  $K_s^0$  candidates are reconstructed in the  $\pi^+ \pi^-$  final states using two different categories. The Long candidates have hits both in the vertex detector and in the tracking stations downstream of the dipole magnet while the Downstream candidates have not track segments in the vertex detector but only in the tracking stations. Events are triggered and selected in a similar way both for the signal modes and the normalisation channel, exploiting the topology of three-body decays and the  $b$ -hadron kinematic properties. Intermediate states containing charmed hadrons are excluded from the signal sample and studied separately.

The decay channel  $\Lambda_b^0 \rightarrow K_s^0 p \pi^-$  is observed for the first time with a significance level of  $8.6\sigma$  and its

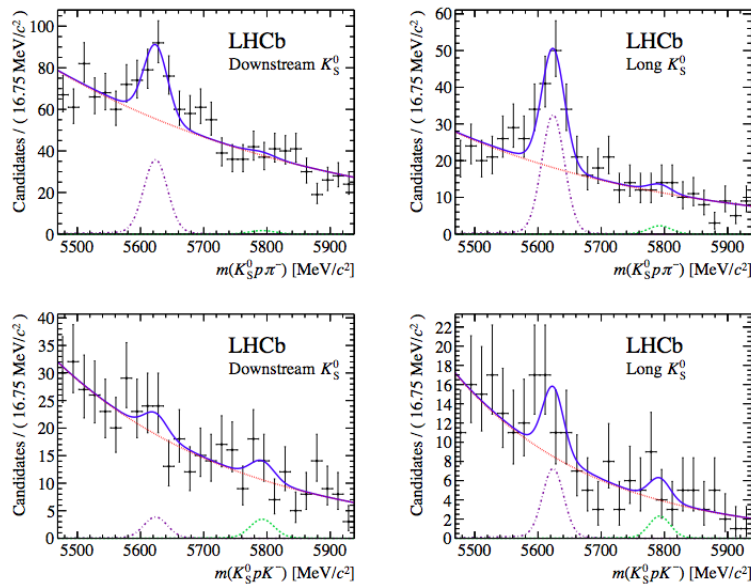


Figure 1: Invariant mass distribution of (top)  $K_s^0 p \pi^-$  and (bottom)  $K_s^0 p K^-$  selected candidates for the (left) Downstream and (right) Long  $K_s^0$  categories.

branching fraction is measured to be

$$\mathcal{B}(\Lambda_b^0 \rightarrow \bar{K}^0 p \pi^-) = (1.26 \pm 0.19 \pm 0.09 \pm 0.34 \pm 0.05) \times 10^{-5},$$

where the first uncertainty is statistical, the second systematic and the third and the fourth related to the uncertainty on the ratio of fragmentation fraction,  $f_{\Lambda_b^0}/f_d$  and on the branching fraction of the  $B^0 \rightarrow K^0 \pi^+ \pi^-$  decay respectively. The CP asymmetry integrated over the phase-space of the observed  $\Lambda_b^0 \rightarrow$

$K_s^0 p \pi^-$  decay is found to be

$$\mathcal{A}^{CP}(\Lambda_b^0 \rightarrow K_s^0 p \pi^-) = 0.22 \pm 0.13 \text{ (stat)} \pm 0.03 \text{ (syst)}.$$

No significant signals are seen for the  $\Lambda_b^0 \rightarrow K_s^0 p K^-$  decay and for the  $\Xi_b^0$  decays and upper limits on their branching fractions are set to

$$\begin{aligned} \mathcal{B}(\Lambda_b^0 \rightarrow \bar{K}^0 p K^-) &< 3.5(4.0) \times 10^{-6} \text{ at 90\% (95\%) CL} \\ f_{\Xi_b^0}/f_d \times \mathcal{B}(\Xi_b^0 \rightarrow \bar{K}^0 p \pi^-) &< 1.6(1.8) \times 10^{-6} \text{ at 90\% (95\%) CL} \\ f_{\Xi_b^0}/f_d \times \mathcal{B}(\Xi_b^0 \rightarrow \bar{K}^0 p K^-) &< 1.1(1.2) \times 10^{-6} \text{ at 90\% (95\%) CL} \end{aligned}$$

### 3 Effective lifetime measurements of the $B_s^0 \rightarrow K^+ K^-$ , $B^0 \rightarrow K^+ \pi^-$ and $B_s^0 \rightarrow \pi^+ K^-$ decays

The effective lifetime measurement of the  $B_s^0 \rightarrow K^+ K^-$  decay, recently measured by LHCb with high precision, is of great interest as it can constrain contributions from new physical phenomena to the  $B_s^0$  system. In addition the  $B^0 \rightarrow K^+ \pi^-$  and  $B_s^0 \rightarrow K^+ \pi^-$  lifetimes, which contribute to the world average of  $\tau(B^0)$  and  $\tau(B_s^0)$ , are measured [3]. The analysis uses a data driven approach to correct for the decay time acceptance introduced by the trigger and the final selection. The procedure consists in extracting the per-event acceptance function directly from data. The effective lifetimes are then determined using a factorised fit to the mass and decay time distributions (see Figure 2). The measured  $B_s^0 \rightarrow K^+ K^-$  lifetime is

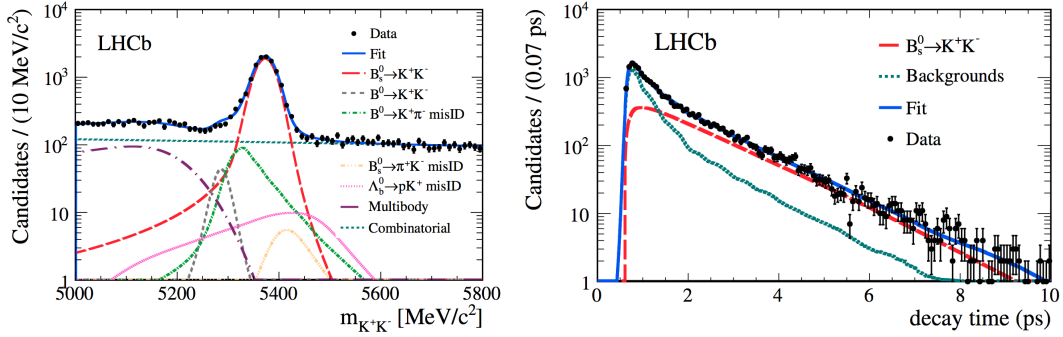


Figure 2: Fit to the  $KK$  invariant mass spectrum and to the reconstructed decay times.

$$\tau_{B_s^0 \rightarrow K^+ K^-} = 1.407 \pm 0.016 \text{ (stat)} \pm 0.007 \text{ (syst)} \text{ ps}$$

which is the world best measurement and is compatible with the SM prediction. The dominant contribution to the systematic uncertainty come from the contamination from misidentified  $B \rightarrow h^+ h'^-$  background channels. The measured lifetimes for  $B^0 \rightarrow K^+ \pi^-$  and  $B_s^0 \rightarrow \pi^+ K^-$  decays are

$$\begin{aligned} \tau_{B^0 \rightarrow K^+ \pi^-} &= 1.524 \pm 0.011 \text{ (stat)} \pm 0.004 \text{ (syst)} \text{ ps} \\ \tau_{B_s^0 \rightarrow \pi^+ K^-} &= 1.60 \pm 0.06 \text{ (stat)} \pm 0.01 \text{ (syst)} \text{ ps} \end{aligned}$$

### 4 Measurement of CP violation in the phase space of $B^\pm \rightarrow K^+ K^- \pi^\pm$ and $B^\pm \rightarrow \pi^+ \pi^- \pi^\pm$

Charmless decays of  $B$  mesons to three hadrons are dominated by quasi-two body processes involving intermediate resonant states. The rich interference pattern makes them favorable for the investigations of CP

asymmetries that are localized in the phase space. Interference between intermediate states of the decay can introduce large strong phase differences which can explain local asymmetries in the phase space [4, 5]. Another explanation focuses on final-state  $KK \leftrightarrow \pi\pi$  rescattering, which can occur between decay channels with the same flavour quantum numbers [5, 6]. CP violation in the phase space of  $B^+ \rightarrow K^+K^-\pi^+$  and  $B^+ \rightarrow \pi^+\pi^-\pi^+$  is measured [7].

Events are selected requiring that the three charged tracks satisfy selection criteria related to their transverse momenta, vertex and track quality. Final state kaons and pions are further selected.

Raw asymmetries are extracted from an unbinned maximum likelihood fit to the mass spectra of the selected candidates and then corrected for detector induced effects and for the  $B^\pm$  meson production asymmetry

$$A_{CP} = A_{\text{raw}} - A_D(\pi^\pm) - A_P(B^\pm)$$

The  $\pi^\pm$  detection asymmetry,  $A_D(\pi^\pm)$ , is calculated using the ratio of full to partially reconstructed  $D^{*+} \rightarrow \pi^+D^0$  decays [8], while the production asymmetry,  $A_P(B^\pm)$ , is evaluated using  $B^\pm \rightarrow J/\psi K^\pm$  decay as control channel. The CP asymmetries are found to be

$$\begin{aligned} A_{CP}(B^\pm \rightarrow \pi^\pm K^+ K^-) &= -0.141 \pm 0.040 (\text{stat}) \pm 0.018 (\text{syst}) \pm 0.007 (A_{CP}(J/\psi K)) \\ A_{CP}(B^\pm \rightarrow \pi^\pm \pi^+ \pi^-) &= 0.117 \pm 0.021 (\text{stat}) \pm 0.009 (\text{syst}) \pm 0.007 (A_{CP}(J/\psi K)) \end{aligned}$$

where the first uncertainty is statistical, the second is the systematic uncertainty and the third is due to the uncertainty on the measurement of the CP asymmetry of the  $B^\pm \rightarrow J/\psi K^\pm$  decay. These measurements represent the first evidence of inclusive CP asymmetries of the  $B^\pm \rightarrow K^+K^-\pi^\pm$  and  $B^\pm \rightarrow \pi^+\pi^-\pi^\pm$  decays with significances of  $3.2\sigma$  and  $4.9\sigma$  respectively.

Asymmetry distributions over the phase space have been studied, as reported in Figure 3, where the raw asymmetries in each bin of the Dalitz plot are shown.

For the  $B^\pm \rightarrow \pi^\pm K^+ K^-$  decays a large negative charge asymmetry is observed in the low  $m_{K^+K^-}^2 < 1.5 \text{ GeV}^2/c^2$

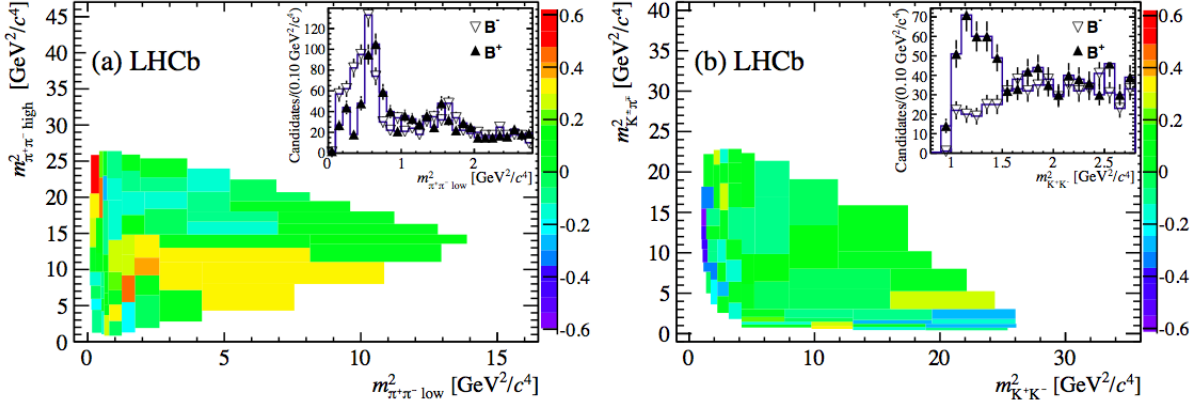


Figure 3: Asymmetries of the number of events in bin of the Dalitz plot for (a)  $B^\pm \rightarrow \pi^\pm \pi^- \pi^+$  and (b)  $B^\pm \rightarrow \pi^\pm K^+ K^-$ . The inset figures show the projections of the number of events in bins of (a)  $m_{\pi^+\pi^-\text{low}}^2 > 15 \text{ GeV}^2/c^2$  and (b) the  $m_{K^+K^-}^2$  variable.

where no resonant contribution is expected. For  $B^\pm \rightarrow \pi^\pm \pi^- \pi^+$  decays, a large positive charge asymmetry is measured in the low  $m_{\pi^+\pi^-\text{low}}^2 < 0.4 \text{ GeV}^2/c^2$  and in the high  $m_{\pi^+\pi^-\text{high}}^2 > 15 \text{ GeV}^2/c^2$ , not clearly associated to a resonant state. Unbinned extended maximum likelihood fits are performed to the mass spectra of the candidates in the regions where large raw asymmetries are found. The local charge asymmetries for the two regions are measured to be

$$\begin{aligned} A_{CP}^{\text{reg}}(B^\pm \rightarrow K^+ K^- \pi^\pm) &= -0.648 \pm 0.070 (\text{stat}) \pm 0.013 (\text{syst}) \pm 0.007 (A_{CP}(J/\psi K)) \\ A_{CP}^{\text{reg}}(B^\pm \rightarrow \pi^+ \pi^- \pi^\pm) &= -0.584 \pm 0.082 (\text{stat}) \pm 0.027 (\text{syst}) \pm 0.007 (A_{CP}(J/\psi K)) \end{aligned}$$

where the first uncertainty is statistical, the second is the systematic uncertainty and the third is due to the uncertainty on the measurement of the CP asymmetry of the  $B^\pm \rightarrow J/\psi K^\pm$  decay. Those results along with recent theoretical developments, may indicate new mechanisms for CP asymmetries [4, 5, 6, 9].

## 5 Measurement of polarization amplitudes and CP asymmetries in $B^0 \rightarrow \phi K^{*0}$ decays

In the Standard Model the  $B^0 \rightarrow \phi K^{*0}$  decay is expected to proceed mainly via a gluonic penguin diagram. For this reason the measurement of CP violation in this decay is sensitive to possible physics beyond the Standard Model, arising in the penguin loop. Since this decay involves a spin-0 B meson decaying into two spin-1 vector mesons, due to angular momentum conservation, there are only three independent configurations of the final state spin vectors. They can be written in term of a longitudinal polarization,  $\mathcal{A}_0$ , and two transverse components with collinear,  $\mathcal{A}_\parallel$ , and orthogonal,  $\mathcal{A}_\perp$ , polarizations.

Angular analyses have shown that the longitudinal and transverse components in this decay have roughly equal amplitudes. Similar results have been observed also in other  $B \rightarrow VV$  transitions in contrast to tree-level decays [10, 11, 12, 13]. The different behaviour of tree and penguin decays has attracted much theoretical attention [14, 15]. In addition to the P-wave amplitudes, there are also contributions where  $K^+K^-$  or  $K^+\pi^-$  are produced in a spin-0 (S-wave) state, ( $A_s^{K^+K^-}$  and  $A_s^{K^+\pi^-}$ ).

Polarization amplitudes and phases are measured by LHCb performing the studies of the angular distributions of the decay products [16]. Candidates are selected from charged tracks with high transverse momentum and impact parameter. Pions and kaons are then selected using particle identification information provided by the RICH detectors. The resulting charged tracks are combined to form  $\phi$  and  $K^{*0}$  meson candidates requiring the invariant mass to be close to the known mass. Kinematic and topological variables are then used in a geometric likelihood method to further suppress background, obtaining about 1800 candidates. A simultaneous fit to the invariant masses and angular observables distributions is performed. The angular analysis results are reported in Table 1. The P-wave parameters are consistent with,

| Parameter                      | Definition  | Fitted value                 |
|--------------------------------|---|------------------------------|
| $f_L$                          | $0.5( A_0 ^2/F_P +  \bar{A}_0 ^2/\bar{F}_P)$  | $0.497 \pm 0.019 \pm 0.015$  |
| $f_\perp$                      | $0.5( A_\perp ^2/F_P +  \bar{A}_\perp ^2/\bar{F}_P)$  | $0.221 \pm 0.016 \pm 0.013$  |
| $f_s(K\pi)$                    | $0.5( A_s^{K\pi} ^2 +  \bar{A}_s^{K\pi} ^2)$  | $0.143 \pm 0.013 \pm 0.012$  |
| $f_s(KK)$                      | $0.5( A_s^{KK} ^2 +  \bar{A}_s^{KK} ^2)$  | $0.122 \pm 0.013 \pm 0.008$  |
| $\delta_\perp$                 | $0.5(\arg A_\perp + \arg \bar{A}_\perp)$  | $2.633 \pm 0.062 \pm 0.037$  |
| $\delta_\parallel$             | $0.5(\arg A_\parallel + \arg \bar{A}_\parallel)$  | $2.562 \pm 0.069 \pm 0.040$  |
| $\delta_s(K\pi)$               | $0.5(\arg A_s^{K\pi} + \arg \bar{A}_s^{K\pi})$  | $2.222 \pm 0.063 \pm 0.081$  |
| $\delta_s(KK)$                 | $0.5(\arg A_s^{KK} + \arg \bar{A}_s^{KK})$  | $2.481 \pm 0.072 \pm 0.048$  |
| $A_0^{\text{CP}}$              | $( A_0 ^2/F_P -  \bar{A}_0 ^2/\bar{F}_P)/( A_0 ^2/F_P +  \bar{A}_0 ^2/\bar{F}_P)$                 | $-0.003 \pm 0.038 \pm 0.005$ |
| $A_\perp^{\text{CP}}$          | $( A_\perp ^2/F_P -  \bar{A}_\perp ^2/\bar{F}_P)/( A_\perp ^2/F_P +  \bar{A}_\perp ^2/\bar{F}_P)$ | $+0.047 \pm 0.072 \pm 0.009$ |
| $A_s(K\pi)^{\text{CP}}$        | $( A_s^{K\pi} ^2 -  \bar{A}_s^{K\pi} ^2)/( A_s^{K\pi} ^2 +  \bar{A}_s^{K\pi} ^2)$                 | $+0.073 \pm 0.091 \pm 0.035$ |
| $A_s(KK)^{\text{CP}}$          | $( A_s^{KK} ^2 -  \bar{A}_s^{KK} ^2)/( A_s^{KK} ^2 +  \bar{A}_s^{KK} ^2)$                         | $-0.209 \pm 0.105 \pm 0.012$ |
| $\delta_\perp^{\text{CP}}$     | $0.5(\arg A_\perp - \arg \bar{A}_\perp)$  | $+0.062 \pm 0.062 \pm 0.006$ |
| $\delta_\parallel^{\text{CP}}$ | $0.5(\arg A_\parallel - \arg \bar{A}_\parallel)$  | $+0.045 \pm 0.069 \pm 0.015$ |
| $\delta_s(K\pi)^{\text{CP}}$   | $0.5(\arg A_s^{K\pi} - \arg \bar{A}_s^{K\pi})$  | $0.062 \pm 0.062 \pm 0.022$  |
| $\delta_s(KK)^{\text{CP}}$     | $0.5(\arg A_s^{KK} - \arg \bar{A}_s^{KK})$  | $0.022 \pm 0.072 \pm 0.004$  |

Table 1: Parameters measured in the angular analysis. The first and second uncertainties are statistical and systematic, respectively. The P- and S-wave fractions are defined as  $F_P = |A_0|^2 + |A_\parallel|^2 + |A_\perp|^2$ ,  $F_P = |A_s^{K\pi}|^2 + |A_s^{KK}|^2$ ,  $F_P + F_s = 1$ .

but more precise than previous measurements and the value of  $f_L$  indicates that longitudinal and transverse polarizations have similar size [17, 18]. Significant S-wave contributions,  $A_s^{K^+K^-}$  and  $A_s^{K^+\pi^-}$ , are found in both the  $K^+\pi^-$  and  $K^+K^-$  systems. The CP asymmetries in both the amplitudes and the phases are consistent with zero. The largest systematic uncertainty on the angular analysis is due to the understanding of the detector acceptance which is determined from simulated events.

## 6 Conclusions

An overview of the latest LHCb results on charmless  $b$ -hadron decays has been given. First observation of  $b$ -baryons decays to hadronic three-body charmless final states has been obtained. The measured effective lifetime in the  $B_s^0 \rightarrow K^+K^-$  decay has been found compatible with the SM expectation. In the  $B^\pm \rightarrow K^+K^-\pi^\pm$  and  $B^\pm \rightarrow \pi^+\pi^-\pi^\pm$  decays, a large CP asymmetry has been found in regions of the Dalitz which do not correspond to resonant contributions. This may indicate new mechanisms for CP asymmetries. More interesting results are expected using the complete 2011 and 2012 available data samples which correspond to an integrated luminosity of  $\sim 3 \text{ fb}^{-1}$ .

## References

- [1] A. A. Alves, Jr. *et al.* [LHCb Collaboration], JINST **3** (2008) S08005.
- [2] R. Aaij *et al.* [LHCb Collaboration], JHEP **1404** (2014) 087 [arXiv:1402.0770 [hep-ex]].
- [3] R. Aaij *et al.* [LHCb Collaboration], arXiv:1406.7204 [hep-ex].
- [4] Z. H. Zhang, X. H. Guo and Y. D. Yang, Phys. Rev. D **87** (2013) 7, 076007 [arXiv:1303.3676 [hep-ph]].
- [5] B. Bhattacharya, M. Gronau and J. L. Rosner, Phys. Lett. B **726** (2013) 337 [arXiv:1306.2625 [hep-ph]].
- [6] I. Bediaga, T. Frederico and O. Loureno, Phys. Rev. D **89** (2014) 094013 [arXiv:1307.8164 [hep-ph]].
- [7] R. Aaij *et al.* [LHCb Collaboration], Phys. Rev. Lett. **112** (2014) 1, 011801 [arXiv:1310.4740 [hep-ex]].
- [8] R. Aaij *et al.* [LHCb Collaboration], Phys. Lett. B **713** (2012) 186 [arXiv:1205.0897 [hep-ex]].
- [9] D. Xu, G. N. Li and X. G. He, Int. J. Mod. Phys. A **29** (2014) 1450011 [arXiv:1307.7186 [hep-ph]].
- [10] P. del Amo Sanchez *et al.* [BaBar Collaboration], Phys. Rev. D **83** (2011) 051101 [arXiv:1012.4044 [hep-ex]].
- [11] J. Zhang *et al.* [BELLE- Collaboration], Phys. Rev. Lett. **95** (2005) 141801 [hep-ex/0408102].
- [12] B. Aubert *et al.* [BaBar Collaboration], Phys. Rev. Lett. **97** (2006) 201801 [hep-ex/0607057].
- [13] R. Aaij *et al.* [LHCb Collaboration], Phys. Lett. B **709** (2012) 50 [arXiv:1111.4183 [hep-ex]].
- [14] A. L. Kagan, Phys. Lett. B **601** (2004) 151 [hep-ph/0405134].
- [15] A. Datta, A. V. Gritsan, D. London, M. Nagashima and A. Szynekman, Phys. Rev. D **76** (2007) 034015 [arXiv:0705.3915 [hep-ph]].
- [16] R. Aaij *et al.* [LHCb Collaboration], JHEP **1405** (2014) 069 [arXiv:1403.2888 [hep-ex]].
- [17] B. Aubert *et al.* [BaBar Collaboration], Phys. Rev. D **78** (2008) 092008 [arXiv:0808.3586 [hep-ex]].
- [18] M. Prim *et al.* [Belle Collaboration], Phys. Rev. D **88**, no. 7, 072004 (2013) [arXiv:1308.1830 [hep-ex]].